EFFECTS OF CO_2 CONDENSATION ON MERIDIONAL MASS FLOWS IN THE WINTER POLAR REGION. K. Ogohara[1] and T. Satomura[1], [1]Division of Earth and Planetary Sciences, Graduate School of Science, Kyoto University, Kyoto, Japan, 606-8502 (ogohara@kugi.kyoto-u.ac.jp)

Introduction: Many local dust storms have been observed near the polar cap edges [1]. Some local dust storms near the polar cap edges grew into a global dust storm [2,3]. Using a GCM, [4] showed that dust artificially injected into the atmosphere near the southern cap edge in the south-west Hellas Basin moved to the north along the western inner rim of the basin. This movement of dust simulated by [4] was relevant to that of the local dust storms which were early aspects of the global dust storm in 2001 reported by [2]. However, their GCM did not take into account the atmospheric mass change due to CO_2 condensation, which would be expected to affect the movement of localized dust near the cap edge.

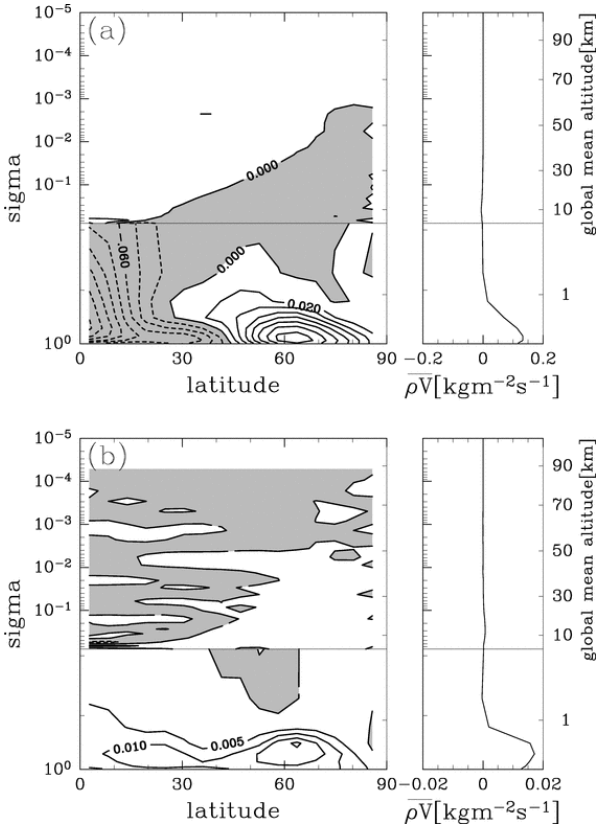

Figure 1: (a) A meridional cross section and a vertical profile, averaged latitudinally from 52.6°N to 69.2°N, of meridional mass flux in S2. Meridional mass flux contours are in intervals of 0.02 kg m^{-2} s^{-1}. (b) Differences of zonal mean meridional mass flux between S1 and S2, which are defined as results in S2 minus those in S1. The contour interval is 0.005 kg m^{-2} s^{-1}. Note that regions below σ=0.8 are stretched vertically. Shaded regions express negative values.

Effects of CO_2 phase-change on surrounding wind fields have been studied by [5] and [6]. [5] estimated the averaged meridional wind associated with the mass flow forced by CO_2 condensation. They considered the growing polar ice cap over the winter pole centered on the pole and supposed that the mass condensing onto the ice cap is continually replenished by a flow into the cylindrical region above the cap. They derived the meridional flow of 0.2--0.5 m s^{-1}, assuming the latent heat due to CO_2 condensation is balanced with radiative cooling. However, they included neither effects of rotation of the planet nor the vertical distribution of the flow. Therefore, it is uncertain whether the picture supposed by [5] is consistent with the real phenomena around the polar cap. On the other hand, [6] evaluated effects of CO_2 phase-change on wind fields by using their MGCM. They concluded that there is any change only at the very lowest level over the cap. However, they mentioned only changes of the meridional distribution of zonal-mean zonal winds caused by CO_2 condensation in the polar region and did not discuss the phenomena associated with the loss of the atmospheric mass due to CO_2 condensation.

In this work, using a numerical Martian atmospheric model, we investigate effects of CO_2 condensation in the winter polar region on the surrounding atmospheric circulation. We perform two kinds of experiments. One is an experiment where the atmospheric mass change due to CO_2 condensation is considered and the other is an experiment where it is not considered. By comparing results of these experiments, effects of CO_2 condensation on the surrounding atmosphere will be suggested.

Model and Experiments: Our MGCM is based on a model used by [4]. The horizontal resolution is approximately 5.6° longitude by 5.6° latitude (triangular truncation with wave number 21). The domain has 34 σ layers in the vertical direction and higher resolution is achieved near the surface. The highest level is at $\sigma_{top}=1.54\times10^{-5}$ corresponding altitudes around 90km. Rayleigh friction is imposed near the upper boundary.

Martian topography is not considered because we are interested only in the responses of the atmosphere to the atmospheric mass change due to CO_2 condensation. The shortwave and longwave radiation scheme used in this work is the same as that used by Ogohara and Satomura [2008] except that atmospheric heating due to absorption of solar radiation in the near-IR bands (4.3, 2.7, 2.0 μm) of CO_2 is computed following

equation (2) given by [7]. The values of the surface albedo of the regolith and CO_2 ice are 0.25 and 0.60, respectively, in all bands.

The time independent vertical profile of dust mixing ratio in the atmosphere given by [8] is used through this work and is the same as that used by [4]. The dust mixing ratio in this work provides the standard dust optical depth about clear atmospheric conditions, ~0.25.

A spin-up run was performed for one Mars year from the northern fall equinox. The one year spin-up run started from an isothermal (220K) condition with constant surface pressure (7hPa) and no wind over the entire planet. During the spin-up run, a temperature adjustment scheme for CO_2 phase-change given by [9] is applied, when the atmospheric temperature falls below the condensation temperature of CO_2. When snow falls on the surface, the mass of the snow is added to the mass of the polar cap. The albedo and the thermal inertia of the surface are switched to those of CO_2 ice. However, the surface pressure is not changed during the spin-up run. After the spin-up run, a simulation called S1 is performed for the period between Ls=180° and Ls=270° on the same conditions as that of the spin-up run. The other simulation called S2 is also performed on the same conditions and for the same period as those of S1 except that the surface pressure is modified based on the snow mass which falls on the surface.

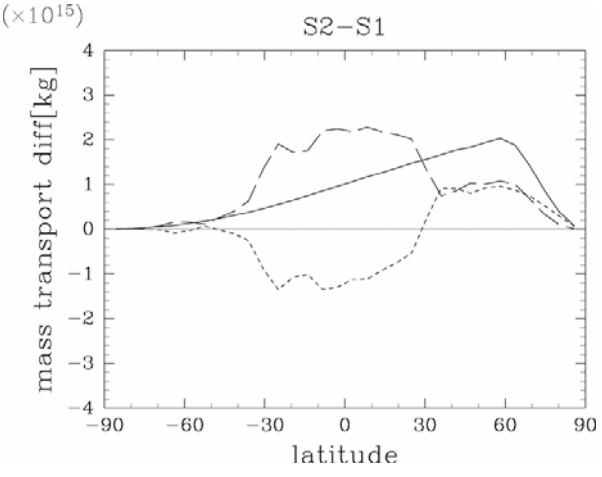

Figure 2: (solid line) Differences of meridional mass transport integrated vertically, longitudinally and temporally between S1 and S2 over the period of the simulations, which are defined as results in S2 minus those in S1. (dashed line) Same as the solid line, but integrated vertically below σ=0.9. (dotted line) Same as the solid line, but integrated vertically above σ=0.9.

Results: A meridional distribution of the zonal-mean meridional mass flux averaged over the period of the simulations in S2 is shown in Fig. 1a. The northerly wind area which lies from the middle atmosphere in high latitudes to the lower atmosphere in low latitudes consists of the lower and descending parts of the Hadley circulation and the descending branch of the Ferrel circulation. It is suggested from an estimation given by [10] that localized meridional mass flux near the surface in high latitudes is the Ekman mass transport. A vertical profile of the zonal mean meridional mass flux in S2 averaged latitudinally from 52.6°N to 69.2°N is also shown in Fig. 1a. Fig. 1b indicates the differences of zonal mean meridional mass fluxes between S1 and S2. Zonal mean meridional mass flux near the surface in high latitudes in S2 is larger than that in S1, associated with the enhancement of the Ekman transport together with the westerly jet enhancement. It is also found in Fig. 1b that the mean meridional circulation is weakened in S2. A vertical profile of the differences of zonal mean meridional mass fluxes averaged latitudinally from 52.6°N to 69.2°N is also shown in Fig. 1b. The significant increase of meridional mass flux can be seen below 1 km altitude in high latitudes. There is also very slight increase of meridional mass flux in altitudes from 10 km to 20 km above the surface.

Discussion and Conclusion: Fig. 2 shows latitudinal distributions of the increase of vertically, longitudinally and temporally integrated meridional mass transport in S2. Considering that the northern ice cap exists in higher latitudes than 60°N, the atmospheric mass transported into the polar region associated with CO_2 condensation in S2 over the period of the simulation is 2.0×10^{15} kg. During the period, the polar ice of 2.4×10^{15} kg is formed (not shown). Thus, about 83 percent of the atmospheric mass lost by CO_2 condensation (i.e. the increment of the polar ice cap mass) is compensated by the northward mass flux from the southern latitudes.

Fig. 2 also shows latitudinal distributions of the differences of the integrated meridional mass transport between S1 and S2. Half of the increment of the northward mass flux in mid- and high-latitudes is contributed from the positive northward mass flux difference above the boundary layer, which corresponds to the slight but vertically wide decrease of the southward mass flux in altitudes between 10 km and 20 km above the surface in S2 shown in Fig. 1, possibly associated with the descending branch of the weakened mean meridional circulation. The other half of the increment of the northward mass flux due to CO_2 condensation is resulted from the increase of the northward mass flux below 1 km altitude. This corresponds to the enhanced

Ekman mass transport shown in Fig 1b. Therefore, the enhancement of Ekman transport is one of important processes of replenishing loss of the atmospheric mass due to CO_2 condensation even if the Ekman layer is very shallow relative to the atmosphere.

As a result, it is summarized that CO_2 condensation affects on the circulation of the surrounding atmosphere as follows,

1)The surface pressure in the polar region drops due to CO_2 condensation onto the surface.

2)The westerly in high latitudes is enhanced uniformly in the vertical direction corresponding to the increase of the meridional gradient of the surface pressure in high latitudes. At the same time, the mean meridional circulation is weakened.

3)The Ekman mass transport in the lower atmosphere is also enhanced together with the westerly jet enhancement and compensates for the loss of the atmospheric mass in the polar region. Weakened mean meridional circulation is resulted in the decrease of the southward mass transport in the descending branch.

Future works: In this work, it is not known exactly how effects of CO_2 phase-change on wind fields appear when topography is considered, because meridional mass transport by topographic stationary waves is not considered in this study. In addition, season of the simulation in this work is the northern fall and winter, when CO_2 continues to condense. The study in the season when CO_2 continues to sublime is the scope of future works.

References:

[1] Cantor, B. A. et al. (2001) *JGR, 106,* E10, 23,653--23,687. [2] Cantor, B. A. (2007) *Icarus, 186,* 60--96. [3]Strausberg, M. J. et al. (2005) *JGR, 110,* E02006, doi:10.1029/2004JE002361. [4] Ogohara, K. and T. Satomura (2008) *Geophys. Res. Lett., 35,* L13201, doi:10.1029/2008GL034546. [5] Read, P. L. and S. R. Lewis (2003) *The Martian Climate Revisited,* Springer. [6] Haberle, R. M. et al. (1993) *JGR, 98,* E2, 3,093—3,123. [7]Forget, F. et al. (1999) *JGR, 104,* E10, 24,155—24,175. [8] Conrath, B. J. (1975) *Icarus, 24,* 36—46. [9]Forget, F. et al. (1998) *Icarus, 131,* 302—316. [10]Stull, R. B. (1997) *An Introduction to Boundary Layer Meteorology,* Kluwer Academic Publishers.